

# Thermal Properties of Graphene–Copper–Graphene Heterogeneous Films

Pradyumna Goli,<sup>†</sup> Hao Ning,<sup>‡</sup> Xuesong Li,<sup>‡</sup> Ching Yu Lu,<sup>‡</sup> Konstantin S. Novoselov,<sup>\*,§</sup> and Alexander A. Balandin<sup>\*,†</sup>

<sup>†</sup>Nano-Device Laboratory, Department of Electrical Engineering, Bourns College of Engineering, University of California – Riverside, Riverside, California 92521, United States

<sup>‡</sup>Bluestone Global Tech, 169 Myers Corners Road, Wappingers Falls, New York 12590 United States

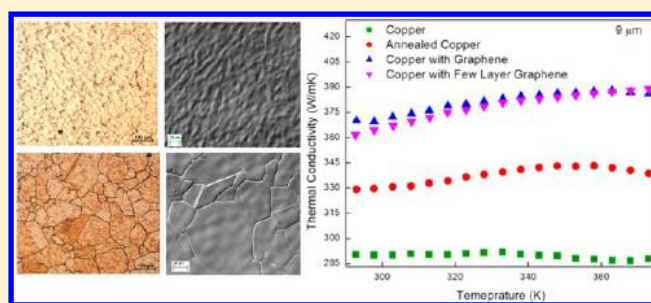
<sup>§</sup>School of Physics and Astronomy, University of Manchester, Oxford Road, Manchester, M13 9PL, United Kingdom

## S Supporting Information

**ABSTRACT:** We demonstrated experimentally that graphene–Cu–graphene heterogeneous films reveal strongly enhanced thermal conductivity as compared to the reference Cu and annealed Cu films. Chemical vapor deposition of a single atomic plane of graphene on both sides of 9  $\mu\text{m}$  thick Cu films increases their thermal conductivity by up to 24% near room temperature. Interestingly, the observed improvement of thermal properties of graphene–Cu–graphene heterofilms results primarily from the changes in Cu morphology during graphene deposition rather than from graphene's action as an additional heat conducting channel.

Enhancement of thermal properties of graphene-capped Cu films is important for thermal management of advanced electronic chips and proposed applications of graphene in the hybrid graphene–Cu interconnect hierarchies.

**KEYWORDS:** Graphene, copper, thermal properties, graphene coating, graphene–copper interconnects, thermal conductivity



Graphene is a one-atom-thick material that is unusual and highly promising for applications of electrical,<sup>1–3</sup> thermal<sup>4,5</sup> and mechanical properties.<sup>6</sup> First obtained by mechanical exfoliation from graphite,<sup>1,2</sup> graphene is now efficiently grown by chemical vapor deposition (CVD) on copper (Cu) films.<sup>7–9</sup> It was reported that layered graphene–metal composites have enhanced mechanical strength.<sup>10</sup> However, it is still not known how the deposition of graphene on Cu films affects the thermal properties of the resulting graphene–Cu films. The knowledge of thermal properties of graphene–Cu “sandwiches” is important for the following practical reasons. Copper became the crucial material for interconnects in silicon (Si) complementary metal-oxide-semiconductor (CMOS) technology by replacing Al. Main challenges with continuous downscaling of Si CMOS technology include electromigration in Cu interconnects, Cu diffusion to adjacent layers, and heat dissipation in the interconnect hierarchies separated from a heat sink by many layers of dielectrics.<sup>11</sup> Combining graphene and Cu in some sort of hybrid heterogeneous global interconnect can bring potential benefits of reducing Cu electromigration and diffusion. It has already been demonstrated that the breakdown current density in prototype graphene interconnects can exceed that in metals by  $\times 10^3$ .<sup>12</sup> Graphene capping of Cu interconnects increases the current density and reduces electrical resistance.<sup>13</sup> Intersecting hybrid graphene–Cu inter-

connects have been shown to offer benefits for downscaled electronics.<sup>14,15</sup> Increasing the heat conduction properties of Cu films with graphene coating could become a crucial added benefit for improving the thermal management of the interconnect hierarchies.

Graphene is known to have usually high intrinsic thermal conductivity, which can exceed that of bulk graphite limit of  $K \approx 2000$  W/mK at RT in sufficiently large high-quality samples.<sup>4,5</sup> However, graphene placement on substrates results in degradation of thermal conductivity to  $\sim 600$  W/mK owing to phonon scattering on the substrate defects and interface.<sup>16</sup> The benefits of using single-layer graphene (SLG) or few-layer graphene (FLG) as heat spreaders for large substrates are not obvious owing to the small thickness of graphene ( $h = 0.35$  nm) and possible thermal conductivity degradation by extrinsic effects. Even if  $K$  is high, the uniform heat flux,  $\Phi = K \times A$ , through the cross-sectional area  $A = hW$  will be small due to small  $h$  ( $W$  is the width of the graphene layer).

In this Letter, we report the results of our thermal measurements that demonstrate that CVD of graphene on both sides of Cu films enhances the thermal diffusivity,  $\alpha$ , and thermal conductivity,  $K$ , of the resulting graphene–Cu–

**Received:** December 19, 2013

**Revised:** February 15, 2014

**Published:** February 20, 2014

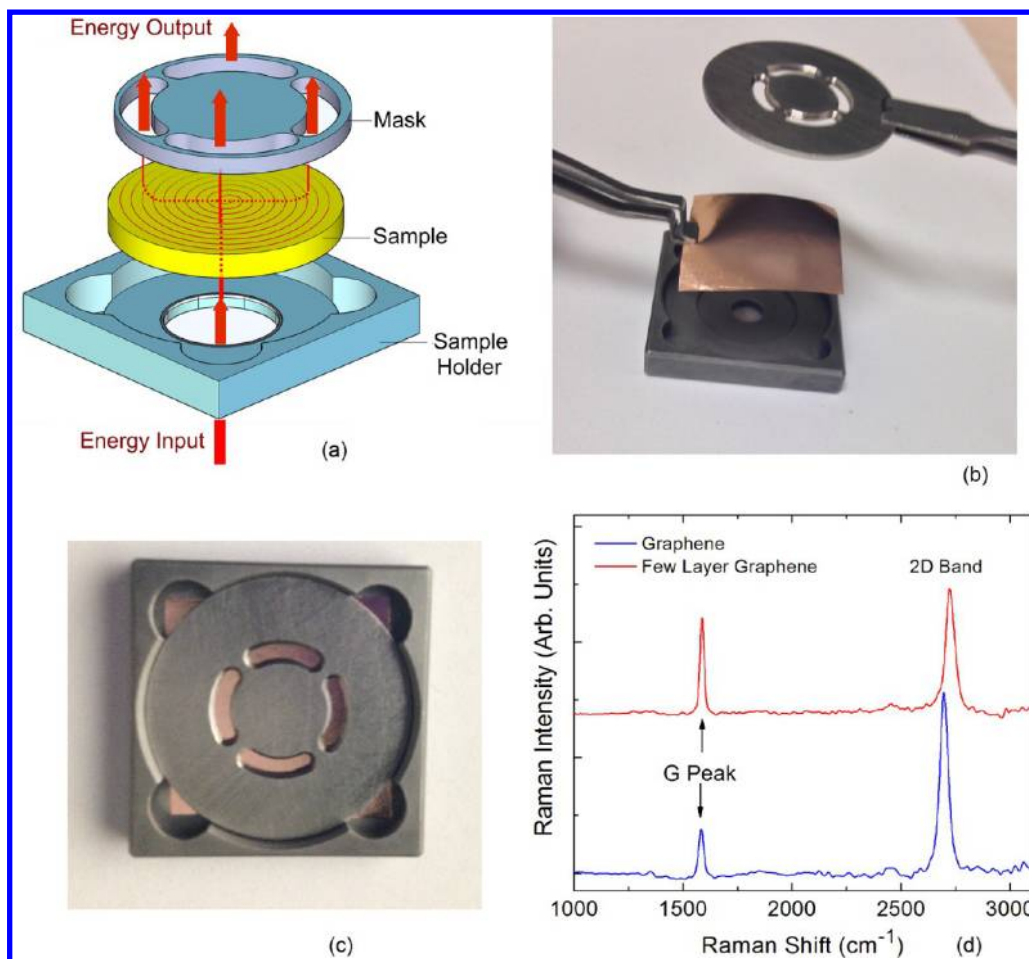


**Figure 1.** Samples and the measurement setup. (a) Schematic of the modified “laser flash” experimental setup for measuring in-plane thermal diffusivity. (b) Cu film coated with CVD graphene placed on the sample holder. (c) Back side of the sample holder with the slits for measuring background subtraction. (d) Raman spectrum of graphene and few-layer graphene on Cu. The data is presented after background subtraction.

graphene (Gr–Cu–Gr) heterofilms. Deposition of graphene increases  $K$  of 9- $\mu\text{m}$  (25- $\mu\text{m}$ ) thick Cu films by up to 24% (16%) near room temperature (RT). Interestingly, the enhancement of thermal properties of Gr–Cu–Gr heterofilms is primarily due to changes in Cu morphology during graphene deposition rather than graphene’s action as an additional heat conducting channel. Specifically, CVD of graphene results in strong enlargement of Cu grain sizes and reduced surface roughness. A typical grain size in Cu films coated with graphene is larger than that in reference Cu films and in Cu films annealed under the same conditions without graphene deposition.

To demonstrate the effect we used a set of Cu films (thickness  $H = 9 \mu\text{m}$  and  $H = 25 \mu\text{m}$ ) with SLG and FLG synthesized on both sides via CVD method (Bluestone Global Tech, Ltd.). As references we used (i) Cu films without graphene or any thermal treatment, and (ii) Cu films annealed under the same conditions as the one used during CVD of graphene. Thus, for comparison we had regular Cu, annealed Cu, Cu with CVD SLG, and Cu with CVD FLG. Details of sample preparation are provided in Methods. The reference Cu, annealed Cu and Cu–graphene samples were subjected to optical microscopy, scanning electron microscopy (SEM), and atomic force microscopy (AFM) inspection. The number of atomic planes in graphene films on Cu was verified with micro-

Raman spectroscopy (Renishaw In Via). Details of our Raman measurement procedures have been reported by some of us elsewhere.<sup>17</sup>

The measurements of the thermal diffusivity were carried out using the “laser flash” method (Netzsch LFA). In conventional configuration, the “laser flash” method gives the cross-plane thermal diffusivity,  $\alpha$ , of the sample.<sup>18</sup> Since we are mostly interested in the in-plane heat spreading properties of Gr–Cu–Gr heterofilms, we altered the experiment by using a special sample holder, which sends the thermal energy along the sample. In this approach, the location for the light energy input on one side of the sample and location for measuring the temperature increase on the other side of the sample are at different lateral positions. The latter insures that the measured temperature increase of the sample corresponds to the thermal diffusivity in the in-plane direction. The thermal conductivity was determined from the equation  $K = \rho\alpha C_p$ , where  $\rho$  is the mass density of the sample and  $C_p$  is the specific heat of the sample measured separately. Details of the measurements are summarized in Methods. Figure 1 presents a schematic of the experiment, an image of a typical sample with the sample holder, and Raman spectra from two different Cu substrates indicating that one has SLG coating while the other has FLG coating. The average thickness of FLG was five atomic planes.

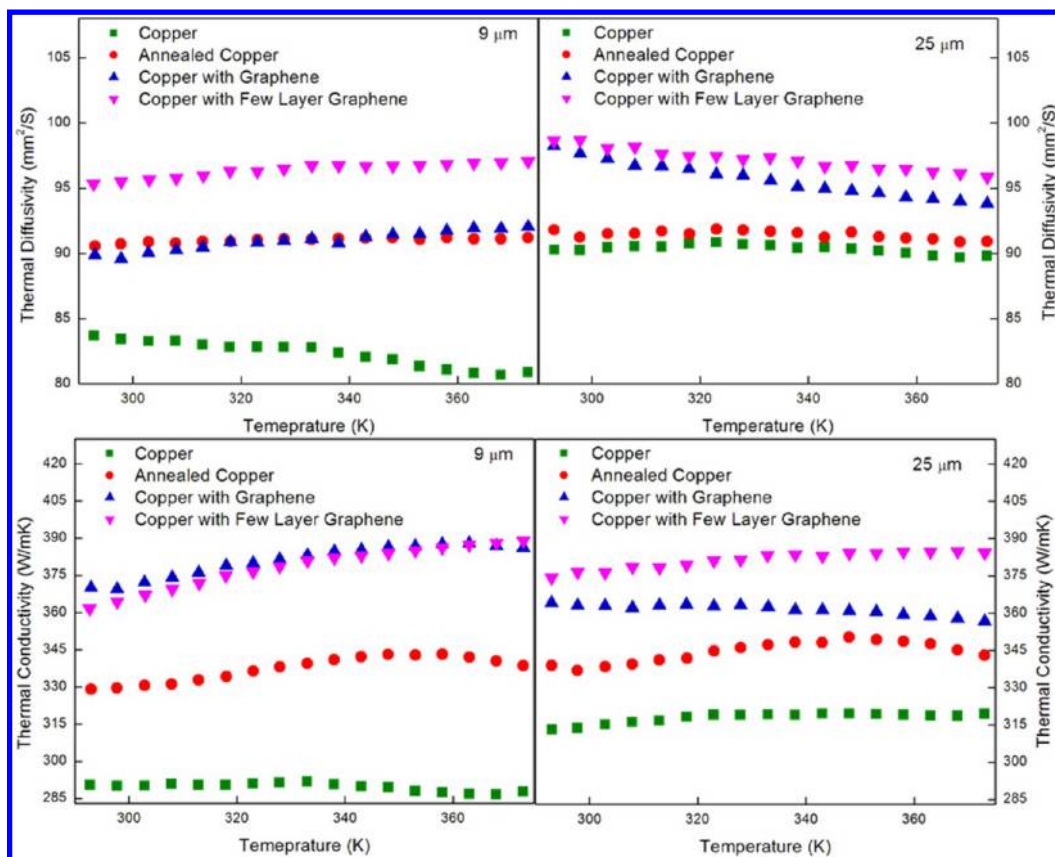


**Figure 2.** Thermal diffusivity and thermal conductivity of graphene-coated copper films. Thermal diffusivity of reference Cu film, annealed Cu, Cu with CVD graphene, and Cu with CVD FLG (top panels). Thermal conductivity of reference Cu film, annealed Cu, Cu with CVD graphene, and Cu with CVD FLG (bottom panels). The data are shown for Cu films with  $H = 9 \mu\text{m}$  and  $H = 25 \mu\text{m}$ . Note that CVD of graphene and FLG results in stronger increase in the apparent thermal conductivity of graphene–Cu–graphene samples than annealing of Cu under the same conditions.

**Table 1.** Thermal Diffusivity and Thermal Conductivity of Graphene Coated Cu Films

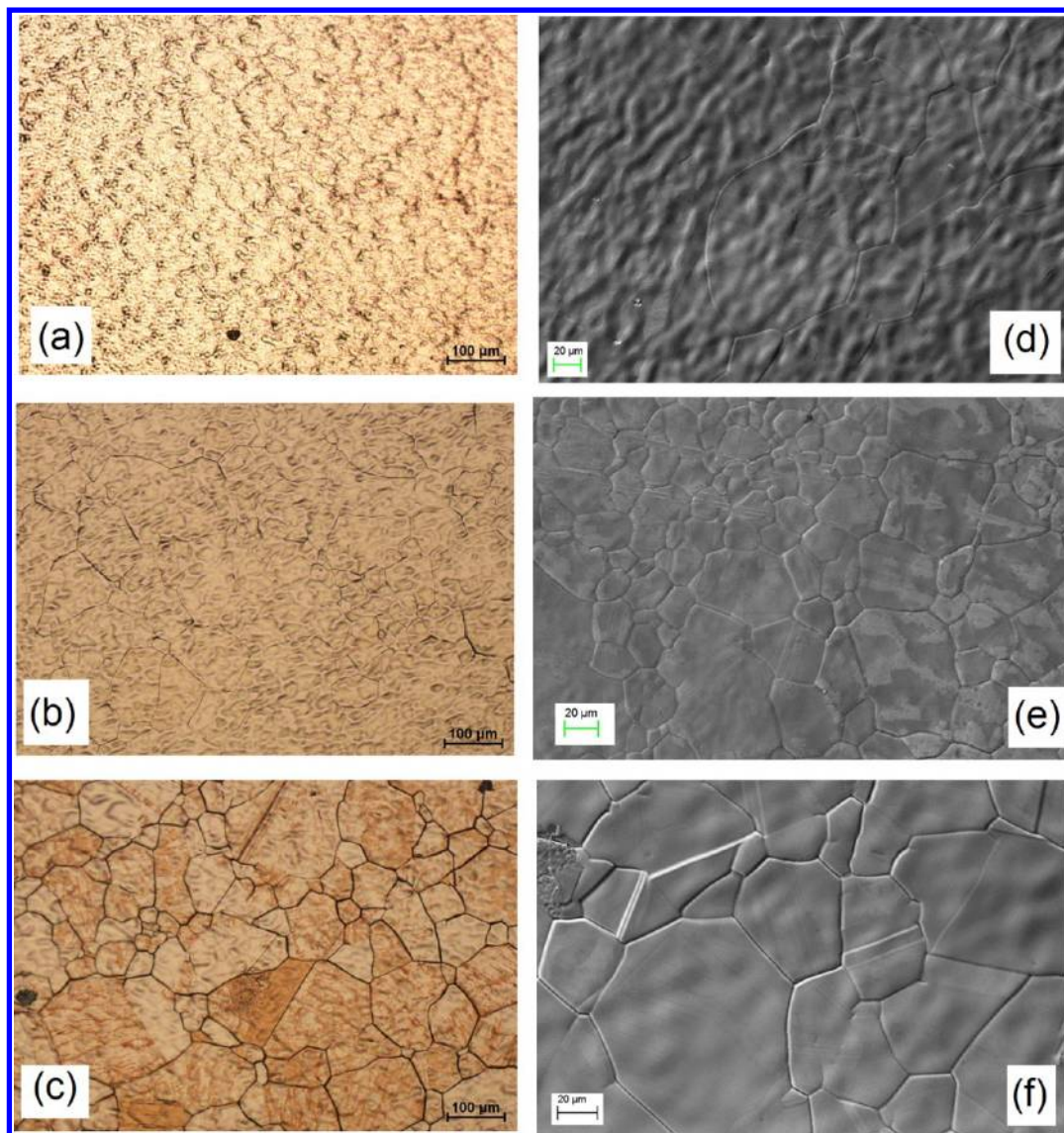
Cu samples	9 $\mu\text{m}$	9 $\mu\text{m}$ annealed	9 $\mu\text{m}$ with SLG	9 $\mu\text{m}$ with FLG	25 $\mu\text{m}$	25 $\mu\text{m}$ annealed	25 $\mu\text{m}$ with SLG	25 $\mu\text{m}$ with FLG
$\alpha$ ( $\text{mm}^2 \text{S}^{-1}$ )	84	90.7 (87–93)	89.6 (88–93)	95.5 (91–99)	90	91.2 (91–92)	97.6 (95–100)	98.4 (98–99)
$K$ (W/mK)	290	329.5 (319–340)	369.5 (361–379)	364.3 (346–378)	313	337.2 (320–358)	363.0 (354–374)	376.4 (372–377)
$\Delta\alpha/\alpha$ (%)		7.4	6.3	12.0		1.3	7.8	8.5
$\Delta K/K$ (%)		11.9	21.5	20.4		7.2	13.8	16.9

Figure 2 presents the average apparent thermal diffusivity and thermal conductivity in reference Cu films, annealed Cu films, Cu films with CVD graphene and Cu films with CVD FLG. The data are presented for two thicknesses of Cu films:  $H = 25 \mu\text{m}$  and  $H = 9 \mu\text{m}$ . The term apparent (another common term is effective) emphasizes that  $\alpha$  and  $K$  values are measured for the whole graphene–Cu–graphene sample. The averaging for each type of sample (e.g., Cu film with SLG) was performed for five locations on each film at each temperature. Two films with the same type of samples were tested. In order to simplify the analyses, in Table 1 we provided the average RT values of  $\alpha$  and  $K$  measured for different samples and locations. The ranges for  $\alpha$  and  $K$  values for different locations and samples are given in the parentheses. The data scatter for different locations was attributed to the sample nonuniformity and film bending, which were unavoidable for large foils (centimeter scale lateral dimensions) with small thicknesses.

The obtained  $\alpha$  and  $K$  of Gr–Cu–Gr heterofilms and their weak temperature dependence are consistent with literature values for bulk Cu, which varies from 385 W/mK to 400 W/mK.<sup>19–21</sup> As reported in refs 20 and 21 in the relevant

temperature range of 300–400 K, the thermal conductivity of copper slightly decreases (increases) in bulk (thin films with  $H \approx 40$ –200 nm range) with temperature. The latter is explained by the interplay of the intrinsic and boundary scattering mechanisms for the heat carriers.<sup>19–21</sup> In terms of their thickness, our samples fall in between these two limiting cases. The latter explains the observed weak and sometimes nonmonotonic dependence of the thermal conductivity on temperature in the examined relatively small temperature range.

Electrons are the main heat carriers in Cu while phonons make the dominant contribution in graphene. The strong reduction of  $K$  of Cu due to electron scattering from the film top and bottom boundaries is only expected in very thin films where the electron mean-free path (MFP) becomes comparable with  $H$ .<sup>21</sup> However, it is known that the grain size in Cu decreases with the decreasing film thickness.<sup>20</sup> For this reason, the size effects can reveal themselves even in relatively thick Cu films with  $H \leq 10 \mu\text{m}$ .<sup>20</sup> The lower  $\alpha$  and  $K$  for 9  $\mu\text{m}$  reference films than those for 25  $\mu\text{m}$  films measured in our experiments are likely related to the grain size effects. The rolling fabrication of Cu films of different thickness (9  $\mu\text{m}$  vs 25  $\mu\text{m}$ ) is also



**Figure 3.** Optical and scanning electron microscopy of Cu and graphene coated Cu. Optical image of the surface of Cu film (a); annealed Cu film (b); and Cu film with CVD graphene (c). SEM image of the surface of Cu film (d); annealed Cu film (e); and Cu film with CVD graphene (f). Note that deposition of graphene substantially increases the Cu grain size.

expected to result in variations in the defect densities, grain elongation and orientation, thus, affecting  $\alpha$  and lowering  $K$ .

The most important and unexpected observation from Figure 2 is that  $\alpha$  and  $K$  are strongly increased in Gr–Cu–Gr heterofilms with graphene or FLG coating compared to reference Cu films or annealed Cu films. Deposition of graphene results in stronger increase of  $\alpha$  and  $K$  than annealing under the same conditions. In terms of thermal conductivity, the effect of graphene deposition is particularly pronounced for thinner Cu films ( $H = 9 \mu\text{m}$ ). The deposition of SLG on  $9 \mu\text{m}$  Cu film results in about  $\sim 22\%$  enhancement of the apparent thermal conductivity as compared to  $\sim 12\%$  increase in the annealed samples without graphene. The average enhancement of  $K$  and  $\alpha$  after deposition of SLG on  $25 \mu\text{m}$  films is less pronounced than that for  $9 \mu\text{m}$  films but still notably larger than for the annealed reference samples. The increase in  $\alpha$  and  $K$  is not proportional because the thermal treatment during CVD or annealing affects the specific heat as well. It is known that thermal treatment of metals and alloys can noticeably

change  $C_p$ , particularly in the presence of impurities and defects.<sup>22</sup>

The overall enhancement of heat conduction properties of Gr–Cu–Gr heterofilms as compared to reference Cu films is very strong and may appear puzzling. The thickness of graphene  $h = 0.35 \text{ nm}$  is negligibly small compared to  $H = 25 \mu\text{m}$ . For this reason, the thermal resistance  $R_\theta = L/(KhW)$  of the additional heat conduction channel via graphene will be much larger than via Cu film (here  $L$  is the length of the path). Thus, the high thermal conductivity of graphene<sup>5</sup> should not play a significant role in heat spreading ability of Cu foils over large distances ( $L \sim 5 \text{ mm}$ ) if one considers conventional heat transfer by phonons. The observed enhancement of the apparent  $\alpha$  and  $K$  can be understood if the thermal data is correlated with the microscopy data presented in Figure 3.

One can see that CVD of graphene results in substantially stronger enlargement of Cu grains than annealing under the same conditions. The graphene CVD and annealing temperature  $1030 \text{ }^\circ\text{C}$  is sufficiently larger than Cu recrystallization temperature of  $\sim 227 \text{ }^\circ\text{C}$ .<sup>23</sup> As a result, annealing accompanied

by recrystallization increases the grain sizes in Cu films, reduces the defect density and improves their mechanical properties.<sup>23,24</sup> Our results indicate that CVD of graphene enhances the Cu grain growth, as compared to regular annealing, by changing the thermal balance during the deposition. Graphene also stops copper evaporation from the surface when the sample is heated during CVD. These conclusions are supported by earlier observations that the substrates and underlays affect the annealing process of Cu and the resulting Cu morphology.<sup>25</sup> It is also in agreement with the grain size data in Cu with CVD graphene and annealed Cu presented in ref.<sup>26</sup> Additionally, our SEM studies indicate that CVD of graphene results in ~20% reduction in surface roughness as compared to reference Cu.

In order to further rationalize the experimental results we estimated the ratio of the average grain sizes,  $\tilde{D}/D$ , which would provide the relative change in the thermal conductivity,  $\Delta K/K$ , close to the one observed in the experiments ( $\tilde{D}$  is typical grain size in reference Cu film and  $D$  is the grain size after CVD of graphene). The electron MFP for thermal transport is  $\Lambda = 40$  nm at RT.<sup>21</sup> Since  $\Lambda \ll H$ , it is reasonable to assume that  $K$  is mostly limited by the grain boundary scattering. In this case, one can express the thermal conductivity,  $K$ , of a polycrystalline metal through that of a single-crystal bulk metal,  $K_B$ , as<sup>21,27–29</sup>  $K = (1 + \Lambda/D)^{-1}K_B$ . Applying this equation to polycrystalline Cu before and after CVD of graphene we derived the following relation

$$\frac{\tilde{D}}{D} = \frac{1 - \left(\frac{\Delta K}{K}\right)}{1 + \left(\frac{\Delta K}{K}\right)\left(\frac{D}{\Lambda}\right)} \quad (1)$$

It is well-known that Cu films have very large distribution of grain sizes.<sup>24,30</sup> It is common to have grain sizes within a given Cu sample varied by three orders of magnitude from tens of nanometers to tens of micrometers.<sup>30</sup> The shape of the grains in the Cu film can also be very anisotropic. Detail investigation of the grain size distribution requires extensive ion-milling and transmission electron microscopy study. For these reasons, here we provide simple estimates from the optical, SEM and AFM studies of our samples. If one assumes that the average grain diameters in Gr–Cu–Gr heterostructures are in the range  $D \approx 1$ – $10$   $\mu\text{m}$ , the experimentally measured  $\Delta K/K = 0.2$  can be achieved for  $\tilde{D}/D$  ranging from ~0.13 to 0.016, which corresponds to the grains in reference Cu on the order of 130–160 nm. Note that the smaller grains can affect the thermal transport the most by limiting the heat carrier MFP. The considered range and change in the diameter by  $\times 10$  to  $\times 100$  after CVD is consistent with the microscopy data (see examples in Figure 3 and Supporting Information). It is known that annealing of Cu under different conditions can change the grain size by many orders of magnitude from ~30 to 100 nm.<sup>24</sup> Deposition of graphene can produce even stronger effect. Thus, our analysis suggests that the grain size increase can result in the observed enhancement of the thermal conductivity. Variations in the defect densities, for example, dislocation lines and grain boundary thickness after CVD of graphene may also affect the  $\Delta K/K$ .

In order to exclude a possibility that the change in thermal conductivity is due to the changes in the impurity content in Gr–Cu–Gr heterofilms and reference annealed Cu films, we performed X-ray photoelectron spectroscopy (XPS) and energy-dispersive X-ray (EDX) spectroscopy inspection. It

was established that the impurity composition (that included O and N) did not differ in graphene–Cu–graphene films with graphene and annealed Cu (Supporting Information). The differences in the grain size and roughness of Gr–Cu–Gr heterofilms and those of annealed Cu films may also be related to differences in the oxidation process during and after CVD of graphene and annealing.<sup>31</sup> One should also note that graphene is an essential for improved thermal conductivity of Gr–Cu–Gr heterofilms. The experiments with deposition of amorphous carbon on Cu indicated that the thermal conductivity has not increased but rather decreased. Amorphous carbon is known to have very low thermal conductivity of below 1 W/mK at RT.<sup>5</sup>

We have also conducted four-probe electrical measurements in order to investigate if the observed change in thermal conductivity in Gr–Cu–Gr heterofilms follows the Wiedemann–Franz law<sup>32</sup>  $K/\sigma = LT$ , where  $\sigma$  is the electrical conductivity and  $L = (\pi^2/3)(k_B/q)^2 \approx 2.44 \times 10^{-8}$  W $\Omega\text{K}^{-2}$  is the Lorenz number. The electrical conductivity of the samples was in line with the tabulated values for Cu films. However, it did not scale up linearly with the measured  $K$  as required by the Wiedemann–Franz law. We explain it by the fact that our samples are heterogeneous, and the electric probes pressed against Gr–Cu–Gr heterofilms contact both graphene or FLG layer and Cu. The electrical conductance is provided by both graphene and Cu channels. As a result, the evolution of electrical conductivity with the change in the grain size does not necessarily correlate well with the apparent thermal conductivity via the Wiedemann–Franz law.

Although it is clear that the observed strong enhancement of thermal properties of Cu films after CVD of graphene is mostly related to the effect produced by graphene on Cu grains one cannot completely exclude other possible mechanisms of heat conduction, which might be facilitated by graphene. It has been recently suggested theoretically that plasmons and plasmon-polaritons can strongly enhance the heat transfer in graphene and graphene-covered substrates.<sup>33,34</sup> In our measurements, the fact that the samples are heated by the light flash with the wide spectrum leaves this possibility open. The plasmon contribution would come in addition to the phonon heat conduction in graphene.

Our present findings add validity to the proposals of the graphene-capped Cu interconnects by demonstrating improvement in their heat spreading ability. Taking into account that the next technology nodes will require Cu interconnects with the nanometers-range thickness<sup>11</sup> one can expect that the effects will be even more pronounced than in the examined micrometers-range thickness films. The latter may become a crucial consideration for electronic industry. In addition, our results can be possibly applied in metallurgy. Carbon additives have long been used in steel smelting as alloying elements distributed through the volume. Carbon alloying allows one to vary the hardness and strength of the metal.<sup>23</sup> Our results show that CVD of one atom thick graphene layer on the surface of metal foils can have a pronounced effect on its thermal properties. This is a conceptually different approach for the carbon use in metallurgy.

In conclusion, we demonstrated experimentally that graphene–Cu–graphene heterogeneous films reveal strongly enhanced thermal conductivity as compared to the reference Cu and annealed Cu films. Chemical vapor deposition of graphene on both sides of 9  $\mu\text{m}$  thick Cu films increases their thermal conductivity by up to 24% near room temperature. The effect of graphene is projected to be substantially stronger in

nanometer thick Cu interconnects. The observed improvement of thermal properties of graphene–Cu–graphene heterofilms results primarily from the changes in Cu morphology during graphene deposition. Enhancement of thermal properties of graphene-capped Cu films is important for thermal management of advanced electronic chips and adds validity to the proposed applications of graphene in the hybrid graphene–Cu interconnects. Our results indicating that deposition of just one atomic plane of graphene on a surface can substantially improve the properties of underlying metal film may lead to a transformative change for the use of carbon in metallurgy.

## METHODS

**Sample Preparation.** The purity of 25  $\mu\text{m}$  thick copper is 99.9% and that of 9  $\mu\text{m}$  thick copper is above 99.99%. Graphene is synthesized in a low-pressure CVD system following the method described in refs 7 and 8. A copper substrate is heated up to 1030  $^{\circ}\text{C}$  under hydrogen and then methane is introduced for graphene growth. The samples with SLG and FLG are synthesized by controlling the cooling rate. For the case of SLG, the copper substrate is cooled from 1030  $^{\circ}\text{C}$  to RT within 20 min while for FLG the cooling time is about 10 h. The annealing of copper for reference samples is performed with the same heating and cooling process as that of SLG synthesis but no methane addition during the process. The annealing time was kept at 20 min.

**Measurement Details.** The “laser flash” technique (LFT) is a transient method that directly measures  $\alpha$ . The specific heat,  $C_p$ , is measured independently with the same instrument using Cu reference. To perform LFT measurement, each sample was placed into a special stage and sample holder (see Figure 1) that fitted its size. The bottom of the stage was illuminated by a flash of a xenon lamp (wavelength  $\lambda = 150\text{--}2000$  nm) with the energy pulse of 1 J for 0.3 ms. The temperature of the opposite surface of the sample was monitored with a cryogenically cooled InSb IR detector. The design of the “in-plane” sample holder ensured that heat traveled  $\sim 5$  mm inside Cu film along its plane, which is a much larger distance than its 25  $\mu\text{m}$  thickness, and thus ensuring the in-plane values for  $\alpha$  and  $K$ . The temperature rise as a function of time,  $\Delta T(t)$ , was used to extract  $\alpha$ . The specific heat,  $C_p$ , was measured with LFT by comparing  $\Delta T(t)$  of the sample to that of a reference sample under the same experimental conditions ( $C_p$  of the reference Cu was  $\sim 0.39$  J/g  $\times$  K at RT). Annealing or CVD of SLG increased  $C_p$ . The increase of specific heat with CVD of graphene or FLG was attributed to morphological changes induced by high temperature during the CVD and the fact that specific heat of graphite,  $C_p = 0.71$  J/g  $\times$  K, is larger than that of Cu. The accuracy of LFT measurement with Netzsch instruments is  $\sim 3\%$ . The thermal conductivity was determined from the equation  $K = \rho\alpha C_p$ , where  $\rho$  is the mass density of the sample.

**Theoretical Analysis Details.** We start with the equation for the thermal conductivity of polycrystalline material limited by the grain boundaries<sup>27–29</sup>

$$K = \left(1 + \frac{\Lambda}{D}\right)^{-1} K_B \quad (2)$$

Here  $D$  is the grain size (mean diameter),  $K_B$  is the thermal conductivity of bulk single-crystal material, and  $\Lambda$  is the electron mean free path (MFP) for thermal transport, which can be larger than that for electrical transport.<sup>27–29</sup> Let us

assume that the material with grain size  $D_1$  has the thermal conductivity  $K_1$  while the material with grain size  $D_2$  has the thermal conductivity  $K_2$ . We introduce two ratios,  $\zeta \equiv (\Delta K/K) = (K_2 - K_1)/K_2 = 1 - K_1/K_2$  and  $\alpha = D_1/D_2$ . Writing eq 2 for two materials with two grain sizes  $D_1$  and  $D_2$ , we get

$$K_1 = \left(1 + \frac{\Lambda}{D_1}\right)^{-1} K_B \quad (3)$$

$$K_2 = \left(1 + \frac{\Lambda}{D_2}\right)^{-1} K_B \quad (4)$$

Dividing eq 3 by eq 4, we can obtain for the thermal conductivity enhancement factor

$$\zeta = 1 - \frac{D_2 + \Lambda}{D_1 + \Lambda} \left(\frac{D_1}{D_2}\right) = 1 - \frac{D_2 + \Lambda}{\alpha D_2 + \Lambda} \alpha \quad (5)$$

Solving eq 5 for  $\alpha$  we get

$$\alpha = \frac{1 - \zeta}{1 + D_2 \left(\frac{\zeta}{\Lambda}\right)} \quad (6)$$

Finally, we obtain the relation between the ratio of the grain sizes and increase in the thermal conductivity

$$\frac{D_1}{D_2} = \frac{1 - \left(\frac{\Delta K}{K}\right)}{1 + \left(\frac{\Delta K}{K}\right) \left(\frac{D_2}{\Lambda}\right)} \quad (7)$$

The derived equation allows one to correlate the effect of increasing grain size in Cu films after graphene deposition with the measured increase in the thermal conductivity. Although the proposed model is simple, it captures the main trend observed experimentally. More accurate treatment requires inclusions of specifics of electron reflections from grain boundaries and external surfaces in polycrystalline films.<sup>35</sup>

## ASSOCIATED CONTENT

### Supporting Information

The Supporting Information provides EDX, specific heat, cross-sectional SEM and additional AFM data for copper, annealed copper and copper with graphene samples. This material is available free of charge via the Internet at <http://pubs.acs.org>

## AUTHOR INFORMATION

### Corresponding Authors

\*E-mail: (A.A.B.) Alexander.Balandin@ucr.edu.

\*E-mail: (K.S.N) Novoselov@manchester.ac.uk.

### Author Contributions

A.A.B. led the thermal data analysis and wrote the manuscript; K.S.N. coordinated the project, contributed to data analysis and manuscript preparation; H.N, X.L., and C.Y.L. prepared the samples; P.G. performed material characterization, thermal measurements, and contributed to data analysis.

### Notes

The authors declare no competing financial interests.

## ACKNOWLEDGMENTS

The work at UC Riverside was supported, in part, by the National Science Foundation (NSF) project ECCS-1307671 on engineering thermal properties of graphene, by DARPA Defense Microelectronics Activity (DMEA) under agreement

number H94003-10-2-1003, and by STARnet Center for Function Accelerated nanoMaterial Engineering (FAME) – Semiconductor Research Corporation (SRC) program sponsored by MARCO and DARPA.

## REFERENCES

- (1) Novoselov, K. S.; et al. Electric field effect in atomically thin carbon films. *Science* **2004**, *306*, 666.
- (2) Novoselov, K. S.; et al. Two-dimensional gas of massless Dirac fermions in graphene. *Nature* **2005**, *438*, 197–200.
- (3) Kim, P.; et al. Experimental observation of the quantum Hall effect and Berry's phase in graphene. *Nature* **2005**, *438*, 201–204.
- (4) Ghosh, S.; et al. Dimensional crossover of thermal transport in few-layer graphene. *Nat. Mater.* **2010**, *9*, 555–558.
- (5) Balandin, A. A. Thermal properties of graphene and nanostructured carbon materials. *Nat. Mater.* **2011**, *10*, 569–581.
- (6) Lee, C.; Wei, X.; Kysar, J. W.; Hone, J. Measurement of the elastic properties and intrinsic strength of monolayer graphene. *Science* **2008**, *321*, 385–388.
- (7) Li, X.; et al. Large-area synthesis of high-quality and uniform graphene films on copper foils. *Science* **2009**, *324*, 1312–1314.
- (8) Li, X.; et al. Graphene Films with Large Domain Size by a Two-Step Chemical Vapor Deposition Process. *Nano Lett.* **2010**, *10*, 4328–4334.
- (9) Mattevi, C.; Kim, H.; Chhowalla, M. A review of chemical vapor deposition of graphene on copper. *J. Mater. Chem.* **2010**, *21*, 3324–3334.
- (10) Kim, Y.; et al. Strengthening effect of single-atomic-layer graphene in metal–graphene nanolayered composites. *Nat. Commun.* **2013**, *4*, 2114.
- (11) Peercy, P. S. The drive to miniaturization. *Nature* **2000**, *406*, 1023.
- (12) Yu, J.; Liu, G.; Sumant, A. V.; Goyal, V.; Balandin, A. A. Graphene-on-Diamond Devices with Increased Current-Carrying Capacity: Carbon sp<sup>2</sup>-on-sp<sup>3</sup> Technology. *Nano Lett.* **2012**, *12*, 1603.
- (13) Kang, C. G.; et al. Effects of multi-layer graphene capping on Cu interconnects. *Nanotechnology* **2013**, *24* (11), 115707.
- (14) Yu, T.; et al. Bilayer graphene/copper hybrid on-chip interconnect: A reliability study. *IEEE Trans. Nanotechnol.* **2011**, *10* (4), 710.
- (15) Chen, Z.; et al. Three-dimensional flexible and conductive interconnected graphene networks grown by chemical vapour deposition. *Nat. Mater.* **2011**, *10*, 424.
- (16) Seol, J. H.; et al. Two-dimensional phonon transport in supported graphene. *Science* **2010**, *328*, 213–216.
- (17) Calizo, I.; et al. Ultraviolet Raman microscopy of single and multilayer graphene. *J. Appl. Phys.* **2009**, *106*, 43509.
- (18) Parker, W. J.; Jenkins, R. J.; Butler, C. P.; Abbott, G. L. Flash method of determining Thermal diffusivity, heat capacity and thermal conductivity. *J. Appl. Phys.* **1961**, *32*, 1679.
- (19) Young, H. D.; Freedman, R. A. *University Physics*, 13th ed.; Addison-Wesley: Reading, MA, 2013; Table 17–5.
- (20) Liu, W.; Yang, Y.; Asheghi, M. In *Thermal and electrical characterization and modeling of thin copper layers*, Intersociety Conference Thermal and Thermomechanical Phenomena in Electronics Systems, San Diego, CA, **2006**; pp 1171–1176.
- (21) Nath, P.; Chopra, K. L. Thermal conductivity of copper films. *Thin Solid Films* **1974**, *20*, 53.
- (22) Przeliorz, R.; Golar, M.; Moskal, G.; Swadzba, L. The relationship between specific heat capacity and oxidation resistance of TiAl alloys. *J. Achiev. Mater. Manuf. Eng.* **2007**, *21*, 47–50.
- (23) Flinn, R. A.; Trojan, P. K. *Engineering Materials and Their Application: Effect of Stress and Temperature*; Houghton Mifflin Company: Boston, MA, 1981; Figures 3–26.
- (24) Gertsman, V. Y.; et al. The study of grain size dependence of yield stress of copper for a wide grain size range. *Acta Metall. Mater.* **1994**, *42* (10), 3539.
- (25) Yang, J.; Hunag, Y.; Xu, K. Effect of substrate on surface morphology evolution of Cu thin films deposited by magnetron sputtering. *Surface Coat. Technol.* **2007**, *201*, 5574.
- (26) Bae, S.; et al. Roll-to-roll production of 30-in. graphene films for transparent electrodes. *Nat. Nanotechnol.* **2010**, *5*, 574–578.
- (27) Qiu, T. Q.; Tien, C. L. Size effects on nonequilibrium laser heating of metal films. *J. Heat Transfer* **1993**, *115*, 842.
- (28) Kumar, S.; Vradis, G. C. Thermal conductivity of thin metallic films. *J. Heat Transfer* **1994**, *116*, 28.
- (29) Zhang, Q. S.; et al. Size effects on the thermal conductivity of polycrystalline platinum nanofilms. *J. Phys.: Condens. Matter* **2006**, *18*, 7937.
- (30) Zielinski, E. M.; Vinci, R. P.; Bravman, J. C. Effects of barrier layer and annealing on abnormal grain growth in copper thin films. *J. Appl. Phys.* **1994**, *76*, 4516.
- (31) Kidambi, P. R.; et al. Observing Graphene Grow: Catalyst-Graphene Interactions during Scalable Graphene Growth on Polycrystalline Copper. *Nano Lett* **2013**, *13*, 4769.
- (32) Franz, R.; Wiedemann, G. Ueber die Wärme-Leitungsfähigkeit der Metalle. *Ann. Phys.* **1853**, *165*, 497.
- (33) Svetovoy, V. B.; VanZwol, P. J.; Chevrier, J. Plasmons enhance near-field radiative heat transfer for graphene-covered dielectrics. *Phys. Rev. B* **2012**, *85*, 155418.
- (34) Ilic, O.; et al. Near-field thermal radiation transfer controlled by plasmons in graphene. *Phys. Rev. B* **2012**, *85*, 155422.
- (35) Mayadas, A. F.; Shatzkes, M. Electrical-resistivity model for polycrystalline films: the case of arbitrary reflection at external surfaces. *Phys. Rev. B* **1970**, *1*, 1382.